DOI: 10.1002/ejic.201100112

Synthesis and Study of the Binuclear μ-Oxodiiron(III) Complexes of 5-Monoaza- and 5,15-Diaza-Substituted β-Octaalkylporphyrins

Pavel A. Stuzhin,*[a] Anwar Ul-Haq,[a] Sergej E. Nefedov,[b] Roman S. Kumeev,[c] and Oscar I. Koifman[a]

Dedicated to Professor Heiner Homborg on the occasion of his 70th birthday

Keywords: Porphyrinoids / Dimerisation / Iron / Bridging ligands

Binuclear μ-oxo-bridged Fe^{III} complexes of 2,3,7,8,12,18-hexamethyl-13,17-dibutyl-5-monoazaporphine [μ-O(FeMAP)$_2$], and 3,7,13,17-tetramethyl-2,8,12,18-tetrabutyl-5,15-diazaporphine [μ-O(FeDAP)$_2$] have been prepared and characterised using UV/Vis, IR and ^{1}H NMR spectroscopies. The stretching vibrations of the μ-oxo-bridge ν_{as}(Fe–O–Fe) are observed at 880 cm^{-1} for μ–O(FeMAP)$_2$ and at 871 cm^{-1} for μ-O(FeDAP)$_2$. The structure of μ-O(FeDAP)$_2$ has been confirmed by the single-crystal X-ray diffraction study of its monobenzene solvate. The Fe1 and Fe2 atoms are displaced from the mean planes formed by the coordinating N-atoms by 0.572 and 0.565 Å, respectively, and are connected to one another through the μ-oxo-bridge. The average Fe1–N and Fe2–N bond lengths are 2.053 and 2.050 Å, and the Fe1–O and Fe2–O bond lengths are 1.777 and 1.776 Å, respectively. The Fe1–O–Fe2 angle is 152.1°, which leads to a non-coplanar arrangement of the two adjacent macrocyclic units (tilt angle 26.3°) allowing for the close approach of the solvating benzene molecule to the bridging oxygen atom with a μ-O···H(benzene) distance of 2.584 Å. Addition of acid HX leads to dissociation of the binuclear μ-oxodiiron complexes and formation of the mononuclear pentacoordinate Fe^{III} complexes (X)FeMAP and (X)FeDAP (X = AcOH, HCl, etc). Analysis of the kinetic results obtained for the reactions of the μ-oxodiiron complexes of (aza)porphyrins with acetic acid in benzene solution indicates that the stability of the μ-oxo bridge towards acid dissociation is primarily determined by its steric accessibility; for species with flexible alkyl chains in β-pyrrolic positions the stability is much lower than in the presence of shielding *meso*- or β-phenyl groups.

Introduction

The ability of synthetic Fe^{III}-porphyrins to form binuclear μ-oxodiiron complexes of the type μ-O(FeP)$_2$, traditionally named μ-oxodimers, has a strong influence on their catalytic properties. Depending on the chemical processes and on the structure of the porphyrin-type ligand, the μ-oxo species can exhibit either enhanced catalytic activity compared with the corresponding mononuclear complex or have no activity at all.[1–6] Thus, the synthesis of μ-oxodimers from various analogues of Fe^{III} porphyrins and the study of their structures, reactivities and stabilities is currently of considerable interest.[7] In the presence of acids HX, the μ-oxo bridge in μ-O(FeP)$_2$ is cleaved and mononuclear pentacoordinate acido complexes (X)FeP are formed. Previously, the kinetics and mechanism of such "dissociation" behaviour have been studied for μ-oxo dimers of the phenyl-substituted Fe^{III} porphyrins *meso*-tetraphenylporphine [μ-O(FeTPP)$_2$][8] and β-octaphenyltetraazaporphine [μ-O(FeOPTAP)$_2$][9] in benzene solution in the presence of acetic and trichloroacetic acids. The synthesis and spectral properties of μ-oxo dimers formed from the β-alkyl-substituted Fe^{III} porphyrins β-octaethylporphine [μ-O(FeOEP)$_2$][10–13] and β-octaethyltetraazaporphine [μ-O(FeOETAP)$_2$][14] have also been reported.

Mononuclear Fe^{III} complexes are also known for forming β-alkylsubstituted *meso*-monoazaporphyrins[15–19] and *meso*-diazaporphyrins,[18–22] however, to the best of our knowledge, their binuclear μ-oxo species have not been characterised. In the present work we report the preparation of new μ-oxodiiron(III) complexes formed from β-alkyl-substituted 5-monoaza- and 5,15-diazaporphyrins [μ-O(FeMAP)$_2$ and μ-O(FeDAP)$_2$; Figure 1], their spectral and structural characterisation and the results of kinetic studies on their stability in benzene solutions in the presence of acetic acid (AcOH).

[a] Department of Organic Chemistry, Ivanovo State University of Chemical Technology,
Friedrich Engels Pr-t, 7, Ivanovo, RF-153000, Russian Federation
E-mail: stuzhin@isuct.ru
[b] Institute of General and Inorganic Chemistry RAS,
Leninskij Pr-t, 31, Moscow, Russian Federation
[c] Institute of Solution Chemistry RAS, ul. Akademicheskaja, 1, Ivanovo, RF-153045, Russian Federation

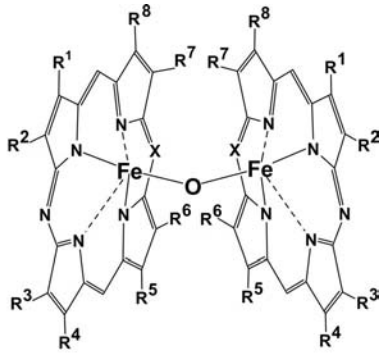

Figure 1. Structural formulae of μ-oxodimers of *meso*-mono- and -diazaporphyrins.

Results and Discussion

Synthesis

The interaction of the free bases H_2AP (AP^{2-} = MAP^{2-} or DAP^{2-}) with iron acetate, formed in situ upon dissolution of iron powder in boiling acetic acid, leads to the corresponding pentacoordinate Fe^{III} complexes [(AcO)-FeAP] with acetate as an axial ligand. During chromatographic purification (from an admixture of unreacted H_2AP) on a column of neutral or basic alumina, the colour changes from the red-brown, typical for pentacoordinate complexes,[22] to green. This is connected with the dimerisation process and formation of the binuclear μ-oxo complexes μ-O(FeAP)$_2$. For other Fe^{III} porphyrins, for example, (X)FeOEP[11,12] and (X)FeOPTAP,[9,23] the formation of the μ-oxo complexes during chromatography of the mononuclear acido complexes was also observed. The structures of μ-O(FeAP)$_2$ have been elucidated on the basis of analytical and spectroscopic data and for the diaza-substituted derivative by a single-crystal X-ray diffraction study.

Crystal Structure

Slow evaporation of a solution of μ-O(FeDAP)$_2$ in benzene led to formation of crystals of the monobenzene solvate μ-O(FeDAP)$_2$·(C_6H_6), which were suitable for X-ray diffraction. The molecular structure is shown in Figure 2 and the crystal-packing diagram in Figure 3. The comparison of the important structural parameters of the coordination environment of the μ-oxo moiety and macrocyclic ligands in μ-O(FeDAP)$_2$ and in the related iron(III) diazaporphyrins and μ-oxodiiron(III) porphyrins are given in Tables 1 and 2.

The two Fe^{III} atoms in μ-O(FeDAP)$_2$ are connected through the μ-oxo bridge with Fe1–O and Fe2–O bond lengths of 1.777 and 1.776 Å, respectively, and an Fe1–O–Fe2 angle of 152.1°. The average Fe–N_{pyr} distance is 2.051 Å; the Fe1 and Fe2 atoms are displaced from the $(N_{pyr})_4$ plane in the direction of the μ-oxo bridge by 0.572 and 0.565 Å, respectively. Such parameters of the coordination pyramid are characteristic of porphyrin complexes in which Fe^{III} is in the high-spin state (S = 5/2).[24] In the complexes with the intermediate (S = 3/2) or admixed (S = 3/2÷5/2) spin states the displacement of Fe^{III} from the plane of the porphyrin macrocycle is much smaller (0.25–0.35 Å) and the Fe–N_{pyr} bond distances are shorter (1.90–2.00 Å), whereas the low-spin complexes (S = 1/2), which

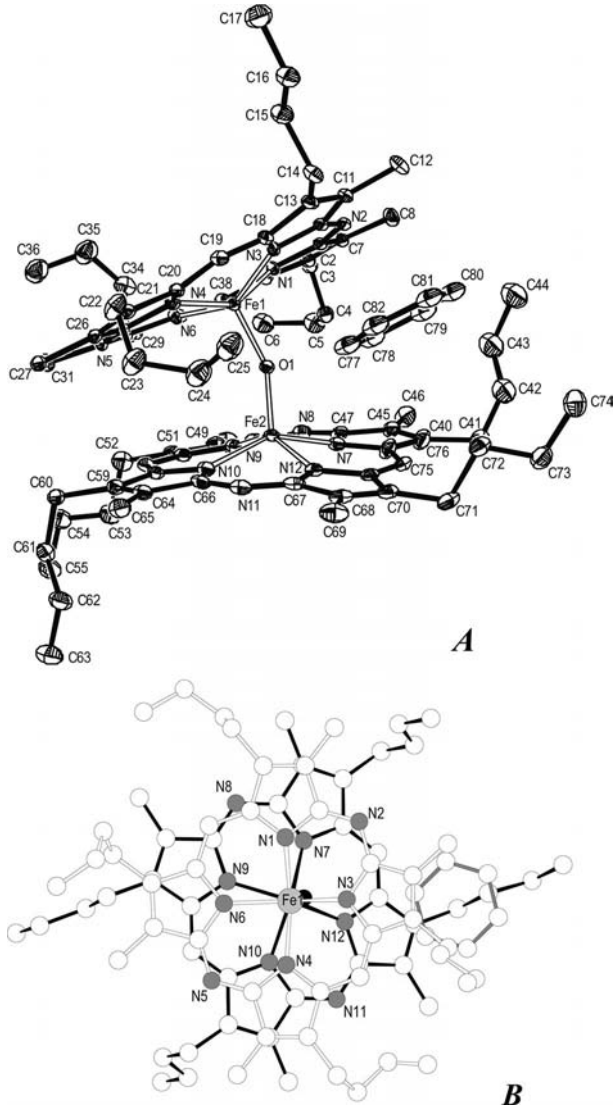

Figure 2. Molecular structure of μ-O(FeDAP)$_2$·(C_6H_6) (*A*) side view with thermal ellipsoids drawn at 30% probability level and (*B*) top view along the Fe1···Fe2 axis. Selected bond lengths [Å] and angles [°]: Fe1–O1 1.777(3), Fe1–N4 2.048(3), Fe1–N1 2.052(3), Fe1–N3 2.054(3), Fe1–N6, 2.056(3), Fe2–O1 1.776(2), Fe2–N7 2.046(3), Fe2–N12 2.048(3), Fe2–N10 2.053(3), Fe2–N9 2.056(3); Fe2–O1–Fe1 152.10(16), O1–Fe1–N1 104.22(12), N1–Fe1–N3 83.84(12), N3–Fe1–N4 87.16(12), N4–Fe1–N6 83.99(12), N1–Fe1–N6 87.21(12), O1–Fe2–N7 106.65(12), N7–Fe2–N9 84.19(13), N9–Fe2–N10 87.18(13), N10–Fe2–N12 84.11(13), N7–Fe2–N12 87.13(13).

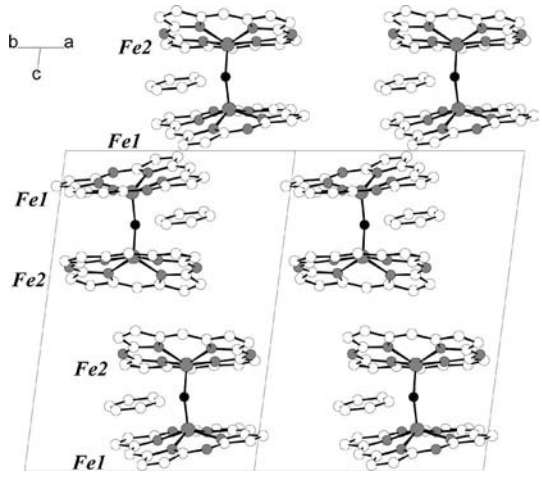

Figure 3. Molecular packing of μ-O(FeDAP)$_2$·(C_6H_6). View along [110] axis. Alkyl groups are not shown for clarity.

are usually hexacoordinate, contain the Fe^{III} atom in the $(N_{pyr})_4$ plane.[24] Thus, in the case of low-spin hexacoordinate Fe^{III} diazaporphyrin $[(L)_2FeDAP]^+ClO_4^-$ (L = 4-cyanopyridine),[21] the Fe^{III} atom is located in the $(N_{pyr})_4$ plane and its withdrawal from this plane in the five-coordinate complex (Cl)FeDAP, which is spin-mixed state (S = 3/2÷5/2), varies from 0.290 to 0.385 Å depending on the contribution of the S = 5/2 state.[22]

The two macrocyclic ligands in μ-O(FeDAP)$_2$ are not coplanar (see Figure 2, *A*); the interplanar tilt angle between the two mean planes $(N_{pyr})_4$ is 28.5° and between the mean planes of two macrocyclic units ∠24/24 is 26.3°. The distance between the Fe1 and Fe2 atoms in the μ-oxodimer is 3.449 Å. The twist angle of two macrocycles in the dimeric unit, determined as a dihedral angle between planes formed by the two *meso*-nitrogen atoms and the Fe atom in each of the fragments, is 74.4° (see Figure 2, *B*). As a result of such molecular conformation, atoms belonging to adjacent macrocycles approach one another by approximately 3.4–3.5 Å on one side of the dimeric molecule ($C_\beta\cdots C_\beta'$ 3.408, $C_\alpha\cdots C_{meso}'$ 3.383, $N_{meso}\cdots C_\alpha'$ 3.508 Å, see Figure 2), whereas on the opposite side, the distance between two C_β atoms located one above the other reach 7.15 Å. This explains the peculiarity of the crystal structure – the presence of the benzene molecule in the cage between the two macro-

Table 1. Selected structural parameters for the μ-oxo complexes of Fe^{III} porphyrins.

Structural parameter[a]	μ-O(FeDAP)$_2$·C_6H_6	μ-O(FeOEP)$_2$				μ-O(FeTPP)$_2$[d]
		triclinic[b]	monoclinic[b]	·C_6H_6·C_{60}[c]		
Fe–O	1.777(3)	1.756(3)	1.755(10)	1.773	1.772	1.763(1)
Fe–N_{pyr}	2.052(6)	2.077(3)	2.080(5)	2.095	2.092	2.087(3)
Δ$(N_{pyr})_4$	0.57	0.48	0.52	0.515	0.513	0.50
∠Fe–O–Fe	152.10(16)	172.2(2)	176.2(2)	150.2(1)	151.9(1)	174.5(1)
∠C_α–X_{meso}–C_α	127.0(C) 122.3(N)	127.4	127.0	126.5	126.5	124.1
∠(N–Fe–Fe–N)	18.9	17.0	16.8	28.3	29.4	35.4
∠(24/24)	26.3	7.3	2.7	27.8	25.0	3.7
N···N(adj)	2.829(C) 2.747(N)	2.858	2.857	2.872	2.869	2.867
N···N(opp)	3.943	4.041	4.039	4.062	4.057	4.054
Fe1···Fe2	3.449(4)	3.503	3.508	3.426	3.437	–

[a] Bond lengths and interatomic distances are given in Å; angles in °. Δ$(N_{pyr})_4$ – displacement of the Fe atom from the $(N_{pyr})_4$ plane; ∠(N–Fe–Fe–N) – dihedral twist angle; ∠(24/24) – tilt angle between mean planes of formed by 24 atoms of two macrocycles in the dimeric unit. [b] Data from ref.[27] [c] Data for two independent molecules from ref.[28] [d] Data from ref.[25]

Table 2. Selected averaged geometrical parameters of the macrocyclic ligand in μ-O(FeDAP)$_2$·(C_6H_6) and structurally related Fe^{III} porphyrin complexes.

Geometrical parameter[a]	μ-O(FeDAP)$_2$·(C_6H_6)	ClFeDAP·$CHCl_3$[b]	$[L_2FeDAP]^+ClO_4^-$[c]	μ-O(FeOEP)$_2$ tri/·(C_6H_6)·C_{60}[d]
C_α–C_{meso}	1.388	1.375	1.382	1.381/1.390
C_α–N_{meso}	1.330	1.326	1.329	–
C_α–N_{pyr}	1.376	1.380	1.383	1.371/1.376
C_α–C_β	1.449	1.447	1.454	1.447/1.453
C_β–C_β	1.355	1.350	1.360	1.357/1.366
∠C_α–N_{pyr}–C_α	105.8	105.5	105.3	106.0/106.0
∠C_{meso}–C_α–N_{pyr}	123.6	124.4	124.0	124.3/124.7
∠N_{meso}–C_α–N_{pyr}	127.5	127.5	127.9	
∠C_α–C_{meso}–C_α	127.0	125.1	125.1	127.4/126.5
∠C_α–N_{meso}–C_α	122.3	121.8	121.5	
N···N(C_{meso})	2.829(C)	2.779(C)	2.775(C)	2.858/2.870
N···N(N_{meso})	2.747(N)	2.717(N)	2.735(N)	
N···N(opp)	3.943	3.887	3.896	4.041/4.060

[a] Bond lengths and distances in Å, bond angles in °. [b] From ref.[22] [c] From ref.[21]; L = 4-cyanopyridine. [d] For the triclinic modification of μ-O(FeOEP)$_2$ from ref.[27] and for the benzene solvate μ-O(FeOEP)$_2$·(C_6H_6)·C_{60} from ref.[28]

cycles. The O···HC distance between the μ-O atom and the benzene H atom (2.584 Å) is less than the sum of the van der Waals radii of the O and H atoms (1.52 + 1.09 = 2.61 Å). The carbon atoms of benzene rings form the shortest contacts of approximately 3.5–3.6 Å with the pyrrolic C_β atoms of the macrocyclic units above and below.

The Fe–O bond lengths in μ-O(FeDAP)$_2$ are very close to the values observed for other μ-oxodiiron porphyrin complexes (Table 1), however, the Fe–O–Fe angle of 152.1° is more than 20° smaller. Thus, the structures of μ-O(FeTPP)$_2$[25,26] and the mono- and triclinic forms of μ-O(FeOEP)$_2$[27] are characterised by an almost linear μ-oxo bridge (∠Fe–O–Fe = 172–176°) and, correspondingly, by an almost coplanar arrangement of the adjacent macrocycles (dihedral angle between the mean planes ∠24/24 = 3–7°). A similar structure with a strongly bent μ-oxo bridge (∠Fe–O–Fe = 148–152°) and a solvent molecule also wedged in the cage between the two non-coplanar porphyrin macrocycles (∠24/24 = 21–28°) has only been seen for μ-O(FeOEP)$_2$ co-crystallised with fullerene C_{60} from benzene[28] and for the *meso*-ethane- or ethylene-linked species {μ-O[FeOEP(*meso*-CH_2-)]$_2$·(PhMe/MeCN), μ-O[FeOEP(*meso*-CH=)]$_2$}·(PhMe) crystallised from toluene or acetonitrile.[7a,7c,7d] Interestingly, for the species with protonated bridged oxygen atom, for example, the μ-hydroxo complex [μ-(HO)(FeOEP)$_2$]ClO_4, the value of ∠Fe–O–Fe is only slightly smaller (146°).[29]

The molecular packing of the dimeric units of μ-O(FeDAP)$_2$ (Figure 3) is affected by intermolecular π-π interaction between concave sides of the macrocycles leading to formation of centrosymmetrical pairs. The parameters of concave–concave overlap of the two macrocycles coordinating Fe1 (interplane distances: 3.40 and 3.51 Å and C_t···C_t' distances: 7.938 and 8.328 Å) according to classification introduced by Scheidt[30] allow only a weak π–π interaction due to partial overlap of pyrrole rings (Figure 4, top). The overlap area between the macrocycles coordinating Fe2 is larger (Figure 4, bottom) and its parameters (interplane distance: 3.67 Å and C_t···C_t': 6.09 Å) are close to the intermediate type of π–π interaction.

Comparison of the selected structural parameters for the macrocyclic units in μ-O(FeDAP)$_2$ and μ-O(FeOEP)$_2$ (Table 2) shows that the substitution of two opposite *meso*-CH groups by *meso*-nitrogen atoms also produces noticeable changes in the structure of the porphyrin ligands. The angles and bond lengths formed by the *meso*-N atoms (∠C_α–N_{meso}–C_α 122.3°, C_α–N_{meso} 1.33 Å) are smaller than that of the *meso*-C atom (∠C_α–C_{meso}–C_α 127.0°, C_α–N_{meso} 1.39 Å). As a result, the angle ∠N_{meso}–C_α–C_β is increased by approximately 4°, the distance between the N-atoms of the pyrrole rings connected by the *meso*-N atoms is reduced by 0.10–0.14 Å and the diameter of the coordination cavity [N···N(opp)] is smaller by approximately 0.10–0.12 Å leading to a larger withdrawal of the Fe ion from the $(N_{pyr})_4$ plane (0.57 vs. 0.50–0.52 Å). Similar changes in the geometry of the macrocycle upon *meso*-diazasubstitution were also observed in other diazaporphyrin complexes with Fe^{III} (see Table 2) and with In^{III}.[31]

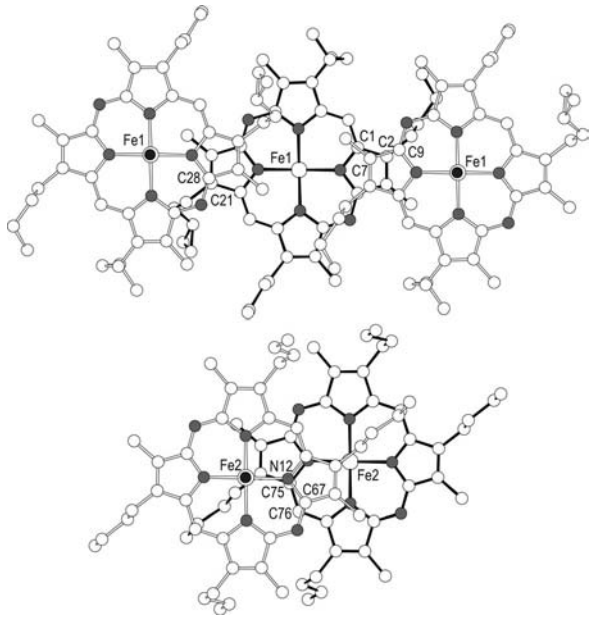

Figure 4. Concave–concave overlap in the centrosymmetrical pairs Fe1···Fe1 (top) and Fe2···Fe2 (bottom) in the crystal structure of μ-O(FeDAP)$_2$·(C_6H_6).

IR Spectra

The IR spectra of the μ-oxodiiron(III) complexes are characterized by the presence of an intense band of asymmetric stretching vibrations of the μ-oxo bridge ν_{as}(Fe–O–Fe) observed at 880 cm^{-1} for μ-O(FeMAP)$_2$ and 871 cm^{-1} for μ-O(FeDAP)$_2$ (see parts *a*,*c* in Figure 5). This band is absent in the IR spectra of the corresponding mononuclear iron(III) complexes with coordinated chloride (Cl)FeAP[22] or acetate moieties (AcO)FeAP (Figure 5, *b*,*d*), which were obtained by the treatment of μ-O(FeAP)$_2$ with hydrochloric or acetic acid (see below). The observed frequencies of the ν_{as}(Fe–O–Fe) vibrations are close to the values reported for μ-oxodiiron(III) complexes of *meso*-tetraphenylporphine, μ-O(FeTPP)$_2$ (870 cm^{-1} [32]) and β-octaethylporphine, μ-O(FeOEP)$_2$ (880 cm^{-1} [11]), but somewhat higher than for the μ-oxodimers of Fe^{III}-tetraphenyl- and Fe^{III}-octaphenyltetraazaporphyrins[33] [841 and 826 cm^{-1} for μ-O(FeTPTAP)$_2$ and μ-O(FeOPTAP)$_2$, respectively].

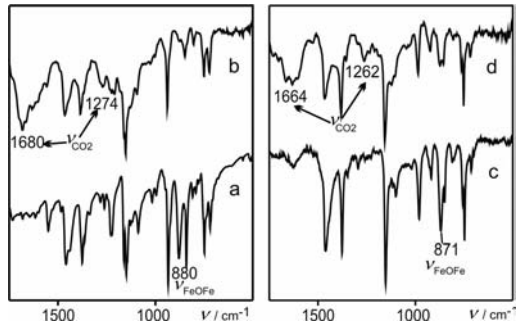

Figure 5. IR spectra of Fe^{III}-monoazaporphyrins (*a*,*b*) and Fe^{III}-diazaporphyrins (*c*,*d*): μ-oxodimers μ-O(FeAP)$_2$ (*a*,*c*) and acetate complexes (AcO)FeAP (*b*,*d*).

^{1}H NMR Spectra

The resonance signals in the ^{1}H NMR spectra of μ-oxo complexes μ-O(FeMAP)$_2$ (Figure 6) and μ-O(FeDAP)$_2$ (Figure 7, *A*) are considerably broadened and shifted compared with the sharp signals in the corresponding free bases (see Table 3) or diamagnetic complexes (e.g., with In^{III} [31,35]). A downfield shift is observed for the resonances of the protons in the α-positions of alkyl groups; the signals of α-CH_3 protons shift from δ = 3.5–3.6 to 5.3–6.0 ppm. The signals for the three non-equivalent α-CH_3 groups in μ-O(FeMAP)$_2$, whilst broadening, become distinctly differentiated ($\Delta\delta$ increases from 0.01 to 0.65 ppm). The signal of the α-CH_2 protons is strongly split ($\Delta\delta$ = 1–1.1 ppm) due to diastereotopy arising from the displacement of the Fe atoms from the macrocyclic plane and is shifted from around δ = 4 ppm in H_2AP and ClInAP ($\Delta\delta < 0.1$ ppm) to δ = 5.4 and 6.3–6.5 ppm. Signals of other butyl protons exerting a slight shift to the opposite high-field direction are observed at δ = 1.9, 1.5–1.6 and 1.1 ppm (for β-CH_2, γ-CH_2 and δ-CH_3, respectively). Signals of the *meso*-CH protons are shifted upfield from around δ = 10 to 5.5–6.5 ppm and, due to broadening, are partly masked by resonances of α-alkyl protons. Such broadening of the resonance signals and their shift compared with the corresponding free bases and diamagnetic metal complexes are characteristic features of the paramagnetism of the central metal atom.[36,37]

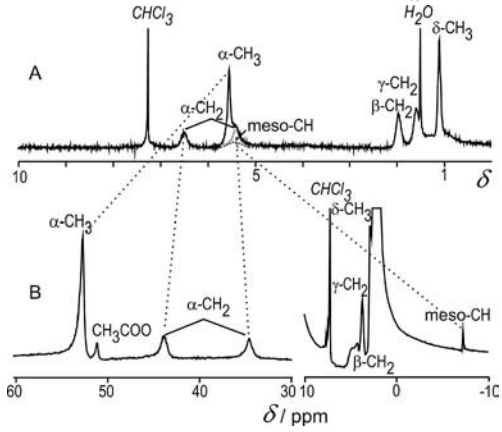

Figure 7. ^{1}H NMR spectra of μ-O(FeDAP)$_2$ in $CDCl_3$ (*A*), in $CDCl_3$ after addition of AcOH (*B*).

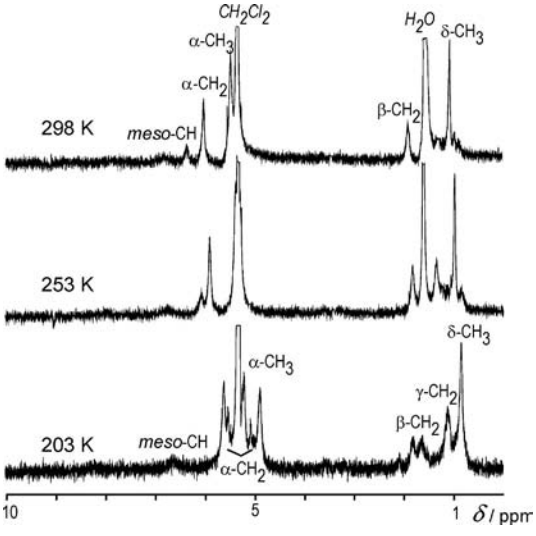

Figure 6. ^{1}H NMR spectra of μ-O(FeMAP)$_2$ in CD_2Cl_2 at 298, 253 and 203 K.

For μ-(oxo)dimers of diamagnetic porphyrin complexes, the resonance signals are not broadened and the shielding effect of the adjacent macrocycle leads only to a slight upfield shift of the protons in the *meso*-positions and in the α-positions of alkyl groups. Thus, in the case of the μ-oxodiscandium(III) complex μ-O(ScOEP)$_2$, the signals of the *meso*-CH protons are shifted upfield by 0.7–1.0 ppm, and the α-CH_2 and α-CH_3 protons by 0.3–0.4 ppm compared with the monomeric complexes (X)ScOEP.[10] In the case of μ-O(FeAP)$_2$, the high-field shift of the *meso*-CH resonances

Table 3. Chemical shifts in the ^{1}H NMR spectra of β-octaalkyl-substituted porphyrin and *meso*-azaporphyrins and their five-coordinate mononuclear and binuclear μ-oxo-bridged iron(III) complexes at ambient temperature.

Porphyrin	Solvent	Chemical shifts (δ, ppm)						Ref.
		meso-CH	α-CH_2	α-CH_3	β-CH_2	β-CH_3	γ-CH_2	δ-CH_3	
H_2OEP	$CDCl_3$	10.18	4.14			1.95			
H_2MAP	CD_2Cl_2	9.92, 10.04	3.99	3.54	2.23		1.75	1.12	[a]
H_2DAP	CD_2Cl_2	9.95	3.97	3.58	2.25		1.76	1.12	[a]
H_2OETAP	$CDCl_3$	–	3.98			1.86			[34]
μ-O(FeOEP)$_2$	$CDCl_3$	6.50	6.03, 5.05			1.75			[11]
μ-O(FeMAP)$_2$	CD_2Cl_2	ca. 6.8 (broad)	6.36, ca. 5.4	6.02, 5.48, 5.36	1.91		1.50	1.07	[a]
μ-O(FeDAP)$_2$	$CDCl_3$	ca. 5.5	6.51, 5.41	5.55	1.96		1.60	1.10	[a]
μ-O(FeOETAP)$_2$	C_6D_6	–	6.59, 5.59			1.80			[14]
(AcO)FeOEP	C_6D_6	–59	38.6		5.9				[48]
	$CDCl_3$	–	39.0, 42.6		6.1				
(Cl)FeOEP	CD_2Cl_2	–56.1	40.9, 44.5		6.7				[46]
(AcO)FeMAP	$CDCl_3$	–27.8 (2 H), –18.4 (1 H)	45.9, 49.6	61.1, 56.3, 49.2	5.7, 4.8		3.9	2.9	[a]
(Cl)FeMAP	CD_2Cl_2	–26.3 (2 H), –17.2 (1 H)	45.4, 48.5	60.0, 55.5, 47.6	5.65, 4.90		4.19	2.79	[a]
(AcO)FeDAP	$CDCl_3$	–7.26	35.3, 44.3	52.7	5.42, 4.25		3.71	2.91	[a]
(Cl)FeDAP	$CDCl_3$	–6.54	32.4, 43.6	51.2	5.08, 4.60		3.92	2.65	[22]
ClFeOETAP	$CDCl_3$		15.3, 38.8		4.06				[14]

[a] This work.

is 2.4–3.4 ppm, and for α-CH_2 and α-CH_3 resonances a shift of 1.3–2.4 ppm to the lower fields is observed. A different direction of the shifts was observed for *meso*-CH- and α-CH_n-protons in μ-O(FeAP)$_2$, evidence that they are primarily determined by the contact mechanism of spin delocalisation from the paramagnetic iron(III) atoms, whereas the influence of the dipole mechanism and the effect of the magnetic anisotropy of the adjacent macrocycles are less important.

The direction and value of the paramagnetic shifts of the *meso*-CH and α-CH_n protons for μ-O(FeAP)$_2$ are similar to those observed for the μ-oxodiiron(III) complexes of octaethylporphine, μ-O(FeOEP)$_2$,[11,29] and octaethyltetraazaporphine, μ-O(FeOETAP)$_2$[14] (see Table 3). Variable-temperature ^{1}H-NMR-spectroscopic measurements revealed a decrease of the isotropic shifts at lower temperatures, that is, *anti*-Curie behaviour [see data for μ-O(FeMAP)$_2$ in Figure 8]. This is characteristic of antiferromagnetic interactions between two Fe^{III} atoms and has also been observed for the μ-oxodiiron(III) complexes of *meso*-tetraphenylporphyrin μ-O(FeTPP)$_2$ and bis(salicylaldimine) μ-O[Fe(salen)]$_2$.[11] Magnetic susceptibility measurements for solid samples of μ-O(FeOEP)$_2$[38] and its ethane-linked derivative μ-O[FeOEP(*meso*-CH_2-)]$_2$[7d] also revealed a strong antiferromagnetic interaction between the two Fe^{III} atoms in the high spin state $S = 5/2$.

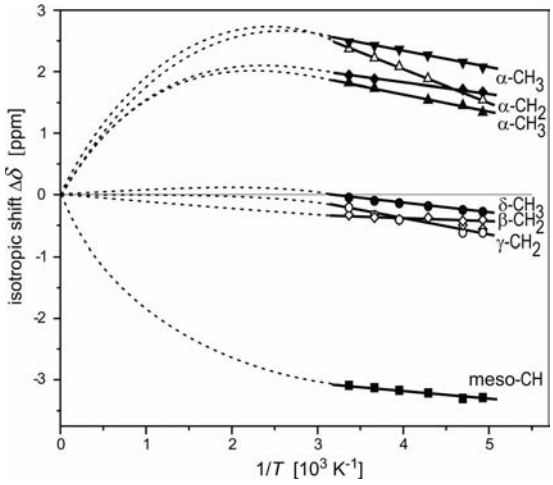

Figure 8. Plot of the temperature dependence of the isotropic shifts for μ-O(FeMAP)$_2$ in $CDCl_3$. The dashed lines illustrates the deviation from Curie behaviour.

UV/Vis Spectra

The UV/Vis spectra of solutions of μ-O(FeAP)$_2$ in neutral solvents (see Figure 1, *a*,*d*) contain two intense π-π* transition bands: a Soret band in the UV region and a *Q*-band in the visible region. Such a spectral pattern is typical for complexes of *meso*-azaporphyrins.[39,40] For the binuclear μ-oxo complexes, the *Q*-band is broadened and the maximum [596 nm for μ-O(FeMAP)$_2$ and 608 nm for μ-O(FeDAP)$_2$] is bathochromically shifted compared with the mononuclear complexes; the maximum of the *Q*-band is observed at 565–580 nm for the Cu^{II} and In^{III} complexes of *meso*-monoaza-substituted porphyrins, CuMAP and (Cl)-InMAP,[35,41] and at 580–595 nm for the *meso*-diaza-substituted species CuDAP and (Cl)InDAP.[31,42] The Soret band maximum in μ-O(FeMAP)$_2$ (351 nm) and μ-O(FeDAP)$_2$ (362 nm) is shifted hypsochromically (385–400 and 375–385 nm in the mononuclear complexes of MAP and DAP, respectively), and has a distinct long-wave shoulder. Such spectral peculiarities observed for μ-O(FeAP)$_2$ might be due to the exciton interaction of two closely located π-chromophores in the binuclear μ-oxo complexes.[43]

In addition, in the series of mononuclear species, *meso*-aza-substitution in μ-oxodiiron complexes of β-octaalkylporphyrins results in the increasing bathochromic shift of the *Q*-band maximum by 6 nm for monoaza-, 18 nm for diaza- and 22 nm for tetraaza-substituted species (Table 4).

Table 4. UV/Vis spectra of the Fe^{III} complexes of β-alkyl-substituted porphyrins and *meso*-azaporphyrins (λ_{max}, nm).

Complex	Solvent	*Q*-band		Soret band
μ-O(FeOEP)$_2$[12]	PhH	590, 563		391
μ-O(FeMAP)$_2$	PhH	596, 559	420 sh	361
μ-O(FeDAP)$_2$	PhH	608, 578 sh	400 sh	350
μ-O(FeOETAP)$_2$[14]	$CHCl_3$	612	579 sh	351
(AcO)FeOEP[48]		616	503, 544	399, 359
(AcO)FeMAP	PhH	641, 602	548, 475	386 sh, 361
(AcO)FeDAP	PhH	678, 621 sh	571, 450	343

It is noteworthy that the spectrum of μ-O(FeMAP)$_2$ is practically identical to the spectrum reported for the Fe^{III} complex of 5-aza-*meso*-porphyrin IX dimethyl ester dissolved in CH_2Cl_2 containing 1% of pyridine (370, 553 and 597 nm).[15] Although the authors believe it to be the chloridoiron(III) complex, the conditions of the described synthetic procedure are more suitable for the formation of the μ-oxo species. Indeed, CH_2Cl_2 used for extraction and aqueous NaCl used for washing were the only possible (but not probable) sources of chloride. Moreover according to our experience, five-coordinate halide complexes of Fe^{III} azaporphyrins are easily hydrolysed to the μ-oxo species under basic conditions (e.g., by water traces in the presence of small additions of pyridine).

Dissociation of Binuclear μ-Oxo Complexes

When a solution of μ-O(FeAP)$_2$ in a non-coordinating solvent (e.g., benzene, chloroform) is acidified by a carboxylic acid or treated with an aqueous solution of a strong mineral acid, a colour change from green to red-brown is observed. Usually, the addition of acid to solutions of *meso*-azaporphyrins leads to reversible spectral changes due to protonation of the *meso*-nitrogen atoms.[35,41,42] The spectral changes observed upon acidification of the μ-O(FeAP)$_2$ solutions can not be reversed when the acid is removed (e.g., by washing of the benzene solution with water). Analysis of the spectroscopic data provide evidence that these colour changes occur due to the rupture of the μ-oxo

bridge and formation of the corresponding five-coordinate acido complexes of Fe^{III}, namely, (X)FeAP according to the following equation:

$$\mu\text{-O(FeAP)}_2 + 2HX \rightarrow 2(X)FeAP + H_2O \quad (1)$$

($X^- = CH_3COO^-$, CF_3COO^-, Cl^-, Br^-, HSO_4^- etc.)

The UV/Vis spectra of the resulting acido complexes (X)FeAP are very characteristic; instead of the *Q*-bands of the initial μ-O(FeAP)$_2$ at 595–610 nm (Figure 9, *a*,*d*), the new broad absorption bands appear at 540–570 and 640–670 nm (Figure 9, *b*,*e*). These also differ greatly from the typical spectra of *meso*-azaporphyrin complexes with M^{II} and M^{III} metals, for example, CuAP,[41,42] ZnAP[39] and (Cl)InAP,[31,35] which contain the intense and sharp *Q*-band in the visible region (Figure 9, *c*,*f*). Analogous spectra were previously reported for the corresponding chloride complexes of Fe^{III} octaethylmonoazaporphyrin, (Cl)FeMAPEt$_8$,[17] and Fe^{III} diazaporphyrin, (Cl)FeDAP.[22] Five-coordinated Fe^{III} complexes of β-octaphenyl- and β-octaethyl-substituted tetraazaporphyrins (X)FeOPTAP[44] and (Cl)-FeOETAP,[14] and Fe^{III} phthalocyanine (X)FePc,[45] and Fe^{III}-porphyrins[46] also have similar spectral features. Such peculiar spectral patterns of five-coordinate Fe^{III} complexes results from the strong interaction between π-orbitals of the macrocyclic azaporphyrin ligand and the partially filled d-orbitals of Fe^{III} in the intermediate (S = 3/2), high (S = 5/2) or mixed (S = 3/2–5/2) spin states. Calculations[47] have shown that, if the Fe^{III} atom has an intermediate or high spin-state (S = 3/2 or 5/2), its d_π orbitals are strongly mixed with π-orbitals of the porphyrin macrocycle. As a result the charge-transfer transitions between the macrocyclic π-MOs and d_π orbitals, and the additional triplet–sextet transitions can gain intensity above and below the *Q*-band.[47]

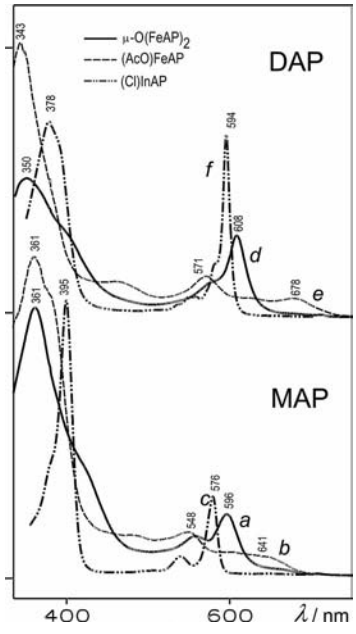

Figure 9. UV/Vis spectra of the Fe^{III} and In^{III} complexes of mono- and diazaporphyrins in benzene: μ-O(FeAP)$_2$ (*a*,*d*), (AcO)FeAP (*b*,*e*) and (Cl)InAP (*c*,*f*).

In the IR spectra of the acetate complexes (AcO)FeAP (Figure 5, *b*,*d*), the bands of the stretching vibration of the μ-oxo-bridge at 870–880 cm^{-1} disappear and two new bands of the carboxylate ν(C=O) and ν(C–O) vibrations appear at 1680 and 1274 cm^{-1} for (AcO)FeMAP and at 1262 and 1664 cm^{-1} for (AcO)FeDAP. For (AcO)FeOEP these vibrations were observed at 1658 and 1285 cm^{-1}.[48] The large difference between the frequencies of these vibrations [$\Delta\nu$(CO) = 402–406 cm^{-1}] clearly indicates the monodentate coordination of the acetate by Fe^{III}.[49] In the case of acetate complexes of Fe^{III}-porphyrins, the difference $\Delta\nu$(CO) is also large (356–409 cm^{-1}) and the monodentate coordination of acetate was established by X-ray crystallography.[48]

^{1}H NMR spectra of μ-O(FeAP)$_2$ also greatly change after the addition of acid leading to the dissociation of the μ-oxo bridge and formation of monomeric acido complexes (X)FeAP. Part *B* of Figure 7 shows the ^{1}H NMR spectrum of (AcO)FeDAP obtained by the addition of acetic acid to a solution of μ-O(FeDAP)$_2$ in $CDCl_3$ until a colour change from green to red-brown was observed. Table 3 displays the proton chemical shifts for the acetate and chloride complexes of monoaza- and diaza-substituted porphyrins [(X)FeMAP and (X)FeDAP, X = AcO, Cl] and for the related pentacoordinate Fe^{III} complexes of β-octaalkylporphyrins. In comparison with the diamagnetic free bases and antiferromagnetically-coupled μ-oxo species, the spectra of (AcO)FeAP are characterized by the strong isotropic shift of the proton resonances due to paramagnetism of Fe^{III}. The signals of the protons in the α-positions of the alkyl groups are strongly shifted to lower field. The singlets of the α-CH_3 groups are observed at 48–60 ppm. The α-CH_2 protons of butyl groups, being diastereotopic due to the out-of-plane position of Fe^{III}, give two signals at δ = 35–50 ppm. The down-field shifts of the protons in the β-, γ- and δ-positions of the butyl groups are considerably smaller and they are observed at δ = 4.2–5.7, 3.7–4.2 and 2.7–2.91 ppm, respectively. The signals of the *meso*-CH protons are shifted in the high-field direction. For the monoaza-substituted complexes (AcO)FeMAP and (Cl)FeMAP, two broad signals (intensity ratio = 1:2) are observed at δ = –17 and –27 ppm, whereas for the diazasubstitited complexes (AcO)FeDAP and (Cl)FeDAP, the sharper signal appears at δ = –7 ppm. The signals at around δ = 52 ppm, which are present in the spectra of the acetate complexes (AcO)-FeAP but are absent for the chloride complexes (Cl)FeAP, can be assigned to the protons of the coordinated acetate in accordance with their integral intensity. Due to the anisotropic effect of the aromatic π-ring current of the azaporphyrin macrocycle, the resonance of the acetate protons is shifted to higher field compared with their positions in the non-aromatic high/intermediate spin Fe^{III} complexes [e.g., δ = 135–140 ppm for the salicylaldimine complexes (AcO)-Fe(salen)[11]].

The isotropic shifts in the ^{1}H NMR spectra of Fe porphyrins are sensitive to the population of the d-orbitals.[36,37,50] Recently we have shown[22] that the splitting of the signals of the diastereotopic protons of the α-CH_2 groups in five-coordinate acido complexes is especially sen-

sitive to the spin state of Fe^{III}. Due to changes in the spin delocalisation mechanism, the splitting increases from 3–4 ppm for purely high-spin (S = 5/2) species to 9–11 ppm for spin mixed (S = 3/2–5/2) and to 31 ppm for the predominantly intermediate spin (S = 3/2) complexes. In the case of the acetate complexes, the monoaza-substituted derivative (AcO)FeMAP with α-CH_2-splitting of 3.7 ppm is a high spin species and diaza-substituted one (AcO)FeDAP (splitting 11 ppm) is a spin-mixed compound.

Stability of μ-Oxo Bridge

To reveal the influence of the structure of the tetrapyrrolic macrocycle on the stability of the μ-oxodiiron complexes in the presence of acid, we have studied the kinetics of the dissociation of μ-O(FeAP)$_2$ in a benzene solution containing 0.001–0.01 M of AcOH. Under these conditions the reaction can easily be followed by spectrophotometry. The observed spectral pattern is characterized by the presence of isosbestic points (Figure 10), which show that only the initial μ-oxo species, having maxima at 590–610 nm, and the resulting monomeric five-coordinate complexes (AcO)-FeAP, with maxima at 650–670 and 550–570 nm, are present in the solution.

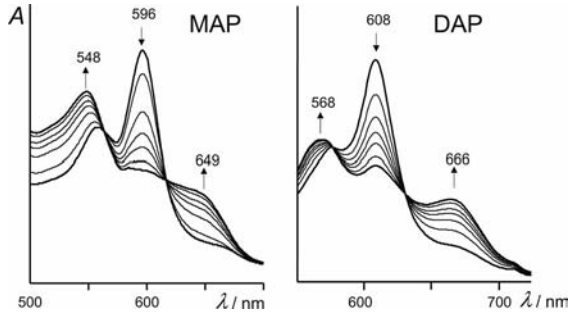

Figure 10. Spectral changes in the visible region observed within 30 min after addition of acetic acid ([AcOH] = 0.003 M) to benzene solutions of μ-O(FeMAP)$_2$ (left) and μ-O(FeDAP)$_2$ (right) at 298 K.

The linear plots of $\ln(c^0/c)$ versus time, which were observed at varying concentrations of acetic acid taken in 1000–10000 fold excess with respect to the μ-oxo species μ-O(FeAP)$_2$ [see Figure 11 for μ-O(FeDAP)$_2$], reveal that the dissociation reaction obeys a pseudo first-order rate law according to the following equation:

$$-dc/d\tau = k_{obs}\,c \quad (2)$$

As can be seen from Table 5, the values of k_{obs} increase with an increase in the concentration of acetic acid. This is also illustrated by Figure 12, which shows the logarithmic dependence of the observed rate constants k_{obs} from the initial concentration of acetic acid $[AcOH]_0$ for the dissociation of μ-O(FeMAP)$_2$ and μ-O(FeDAP)$_2$ in benzene solution at 298 K. For comparison, this figure also includes the data for the μ-oxodiiron(III) complexes of *meso*-tetraphenylporphine [μ-O(FeTPP)$_2$][8] and β-octaphenyltetraazaporphine [μ-O(FeOPTAP)$_2$][9] studied previously. In all cases, the slope of the logarithmic dependence is close to 1. It should, however, be noted that acetic acid is substantially dimerised in benzene solution:

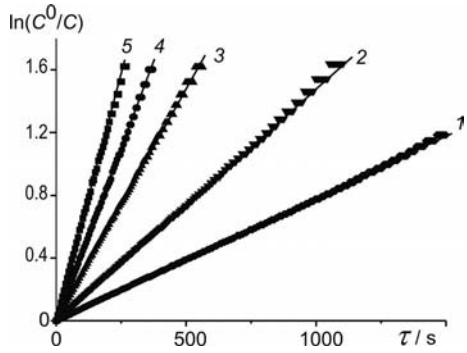

Figure 11. Time dependences of $\ln(c^0/c)$ for the dissociation of μ-O(FeDAP)$_2$ in benzene in the presence of acetic acid at 298 K. [AcOH] = 0.01191 (*1*), 0.00893 (*2*), 0.00596 (*3*), 0.00298 (*4*) and 0.00119 M (*5*).

$$2AcOH = (AcOH)_2,\ K_D = [AcOH_D]/[AcOH_M]^2 \quad (3)$$

The value of the dimerization constant K_D at 298 K in benzene, determined by calorimetry, is 462 ± 108 M^{-1}[51] and the more recent value obtained by IR spectroscopy is 390 ± 70 M^{-1}.[52] In the studied concentration range of acetic acid (0.001–0.01 M), the content of acetic acid in the monomeric and dimeric forms is comparable (66% of monomer in 0.001 M and 30% in 0.01 M solutions) and they can both act as an active species in the dissociation of μ-oxo complexes:

$$\mu\text{-}O(FeAP)_2 + AcOH \rightarrow (AcO)FeAP + (HO)FeAP\ (k_M) \quad (4)$$

$$\mu\text{-}O(FeAP)_2 + (AcOH)_2 \rightarrow 2(AcO)FeAP + H_2O\ (k_D) \quad (5)$$

In this case the following expression for k_{obs} should be valid:

$$k_{obs} = k_M[AcOH_M] + k_D[AcOH_D] \quad (6)$$

or taking into account the expression (3) for K_D:

$$k_{obs} = k_M[AcOH_M] + k_D\,K_D[AcOH_M]^2 \quad (7)$$

$$k_{obs}/[AcOH_M] = k_M + k_D\,K_D[AcOH_M] \quad (8)$$

From the linear dependence of $k_{obs}/[AcOH_M]$ from $[AcOH_M]$ (Figure 13) using the linearized form (8) of the Equation (7) and the value of K_D = 390 M^{-1} in benzene at 298 K,[52] we have calculated the constants of the dissociation reaction under action of monomeric and dimeric acetic acid (k_M and k_D, see Table 5).

The dimeric form of acetic acid appeared to be approximately 1.4 times more active in dissociation than the monomeric one: for μ-O(FeMAP)$_2$ k_M = 1.71 $s^{-1}M^{-1}$ and k_D = 2.33 $s^{-1}M^{-1}$, and for μ-O(FeDAP)$_2$ k_M = 1.47 $s^{-1}M^{-1}$ and k_D = 2.04 $s^{-1}M^{-1}$. Since, in the studied concentration range of acetic acid, the monomer to dimer ratio changed from 1.51 to 0.73 for μ-O(FeMAP)$_2$ and from 3.42 to 0.77 for μ-O(FeDAP)$_2$, one can conclude that reactions (4) and (5)

Table 5. Kinetic parameters of dissociation of μ-O(FeMAP)$_2$ and μ-O(FeDAP)$_2$ in benzene in the presence of acetic acid.

[AcOH] [M]	Monomer[a] [$AcOH_M$], 10^{-3} M	Dimer[a] [$AcOH_D$], 10^{-3} M	$10^3 k_{obs}$, s^{-1} 298 K	308 K	323 K
			μ-O(FeMAP)$_2$		
0.00393	1.693	1.118	5.58 ± 0.03		
0.00524	2.029	1.606	7.12 ± 0.05		
0.00786	2.597	2.631	10.03 ± 0.07	13.65 ± 0.08	21.3 ± 0.18
0.0105	3.084	3.708	13.42 ± 0.09	18.07 ± 0.15	29.96 ± 0.72
0.0131	3.507	4.797	17.76 ± 0.11	26.17 ± 0.25	40.72 ± 0.47
			k_M = 1.71 ± 0.27 $s^{-1}M^{-1}$	E_a = 26± 3 kJ mol^{-1}	
			k_D = 2.33 ± 0.26 $s^{-1}M^{-1}$	$\Delta S^{\#}$ = –205 ± 10 J mol^{-1} K^{-1}	
			μ-O(FeDAP)$_2$		
0.00119	0.751	0.220	1.69 ± 0.01		
0.00298	1.416	0.782	3.44 ± 0.02	6.78 ± 0.02	17.75 ± 0.18
0.00596	2.197	1.882	6.83 ± 0.03	12.06 ± 0.10	28.09 ± 0.48
0.00893	2.803	3.064	10.13 ± 0.07	17.63 ± 0.20	37.99 ± 1.09
0.01191	3.319	4.296	14.21 ± 0.10	27.67 ± 0.36	48.95 ± 1.42
			k_M = 1.47 ± 0.21 $s^{-1}M^{-1}$	E_a = 45 ± 3 kJ mol^{-1}	
			k_D = 2.04 ± 0.24 $s^{-1}M^{-1}$	$\Delta S^{\#}$ = –155 ± 10 J mol^{-1} K^{-1}	

[a] Concentration of the monomer and dimer is calculated using the dimerization constant of acetic acid in benzene K_D = 390 M^{-1} from ref.[52]

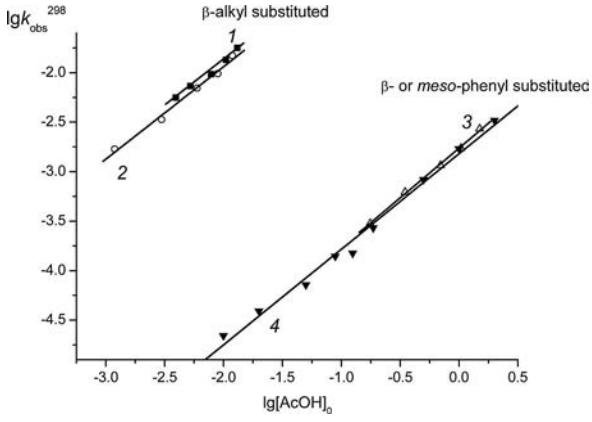

Figure 12. Logarithmic plots of the rates constants versus concentration of acetic acid for dissociation of the μ-oxodiiron(III) complexes of β-alkyl- (*1*,*2*) and β- or *meso*-phenyl-substituted (*3*,*4*) porphyrins and azaporphyrins in benzene at 298 K. *1* = μ-O(FeMAP)$_2$, *2* = μ-O(FeDAP)$_2$, *3* = μ-O(FeOPTAP)$_2$, *4* = μ-O(FeTPP)$_2$.

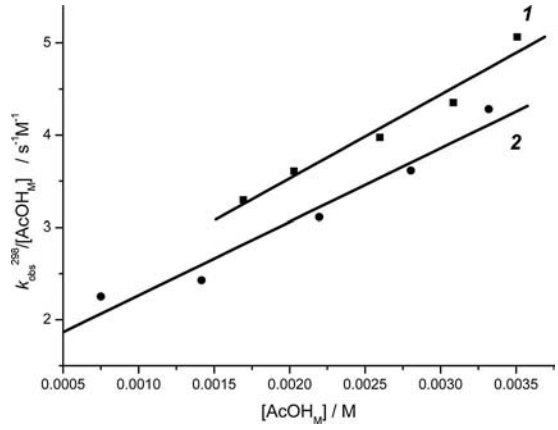

Figure 13. Dependences of k_{obs}/[$AcOH_M$] from [$AcOH_M$] for the dissociation of μ-O(FeMAP)$_2$ (*1*) and μ-O(FeDAP)$_2$ (*2*) in benzene in the presence of acetic acid at 298 K.

contribute comparably in the dissociation of these μ-oxo species. A comparison of the k_M and k_D values for μ-O(FeMAP)$_2$ and μ-O(FeDAP)$_2$ indicates that the introduction of an additional *meso*-nitrogen atom only slightly increases the stability of the μ-oxo dimers to dissociation in acid media.

It is also interesting to compare the data obtained on the stability of the μ-oxo dimers of alkyl-substituted Fe^{III} *meso*-azaporphyrins with the kinetic data previously reported for the *meso*- and β-phenyl-substituted species, μ-O(FeTPP)$_2$ and μ-O(FeOPTAP)$_2$, which were also obtained in benzene–AcOH solutions.[8,9] Using the original kinetic data for these species and the dimerization constant K_D^{298} = 390 M^{-1}, we have calculated the rate constants for μ-O(FeTPP)$_2$ (k_M = 0.000815 c^{-1} M^{-1} and k_D = 0.00335 c^{-1} M^{-1}) and for μ-O(FeOPTAP)$_2$ (k_M = 0.00356 c^{-1} M^{-1} and k_D = 0.000478 c^{-1} M^{-1}). These values differ somewhat from the k_M and k_D values reported in the original publications[8,9] as the value K_D^{298} = 800 M^{-1}, obtained by an indirect method, was used.[53] It can be seen by comparison of the k_M and k_D values, and especially from Figure 12, that *meso*-azasubstitution in the porphyrin macrocycle has almost negligible influence on the stability of the μ-oxo complexes. At the same time the peripheral phenyl substitution in the *meso*- or in the β-positions increases the stability in an acidic medium by almost three orders of magnitude. This indicates that the dissociation rate of μ-oxodiiron porphyrin complexes in the presence of acetic acid is determined by steric shielding of the μ-oxo bridge and not by electronic factors due to *meso*-azasubstitution in the macrocycle. Unlike *meso*- and β-phenyl-substituted species, in the case of β-alkyl-substituted macrocycles the μ-oxo bridge appeared to be more easily accessible for the interaction. This is in the agreement with the available structural data illustrating that β-octaalkyl groups can allow bending of the μ-oxo bridge making it more open for the interaction (e.g., with benzene molecules).

One can suppose that dissociation reactions (4) and (5) proceed through formation of the bridged intermediate states, μ-hydroxo-μ-acetate $[(APFe)\mu\text{-}(HO)\mu\text{-}(AcO)\text{-}(FeAP)]^{\neq}$ or μ-aqua-μ-diacetate $[(APFe)\mu\text{-}(H_2O)\mu\text{-}(AcO)_2\text{-}(FeAP)]^{\neq}$, respectively, or through structurally similar intermediates. Formation of the stable μ-hydroxo-μ-(di)acetate Fe^{III} complexes was observed for the derivatives of 1,4,7-trimethyl-1,4,7-triazacyclononane (L) $\{(\mu\text{-OH})(\mu\text{-AcO})_2\text{-}[Fe(L)]_2\}^{-}$[54] and hydrotris(1-pyrazolyl)borate (L′) $\{\mu\text{-}(HO)(\mu\text{-AcO})_2[Fe(L')]_2\}^{+}$.[55] In the case of Fe^{III} porphyrins, stable complexes with only one bridge (μ-oxo and μ-hydroxo) are known. Evidently, a rigid and bulky porphyrin macrocycle does not allow formation of stable doubly- and triply-bridged structures, which can be formed only in the transition state. The strongly negative values of the entropy of activation $\Delta S^{\#}$ [-205 ± 10 for μ-O(FeMAP)$_2$ and -155 ± 10 J mol^{-1} K^{-1} for μ-O(FeDAP)$_2$] indicate that the reaction most probably occurs through a bridged transition state and not through a bridged intermediate.

Conclusion

Binuclear μ-oxodiiron(III) complexes of *meso*-monoaza- and *meso*-diaza-substituted β-octaalkylporphyrins have been synthesized and their structure and physico-chemical properties have been studied by UV/Vis, IR and ^{1}H NMR spectroscopic measurements. The presence of the μ-oxo bridge is evidenced by appearance of its asymmetric stretching vibration in the IR spectra and for *meso*-diaza-substituted species confirmed by single-crystal X-ray diffraction analysis. Conformational flexibility of the alkyl groups allows a non-coplanar arrangement of the macrocyclic units and substantial bending of the μ-oxo bridge facilitating its solvation by a benzene molecule as is evidenced by the X-ray study. As a consequence dissociation of the present μ-oxo dimers in the presence of acetic acid occurs much more easily compared with μ-oxodiiron(III) complexes of *meso*- and β-phenyl-substituted porphyrin macrocycles in which the steric interaction between phenyl groups requires an almost coplanar arrangement of the adjacent macrocycles; the μ-oxo bridge is almost linear and less accessible for an attack of acid.

Experimental Section

Measurements: Electronic absorption spectra were recorded with a Hitachi U-2000 spectrophotometer using 10^{-6}–10^{-5} M solutions of complexes. IR spectra were registered on FT-IR spectrometers NIC 5DXB and Avatar-360 for samples in KBr. ^{1}H NMR spectra were measured on Bruker AC200 spectrometer. Elemental analysis were performed on CHNS-O Analyser Flash EA 1118 Fa. Thermo Quest.

Materials: Commercially available solvents were dried according to conventional procedures and distilled prior use. The free bases H_2MAP[56] and H_2DAP[57] were prepared by the previously reported methods.

μ-Oxo-bis[13,17-dibutyl-2,3,7,8,12,18-hexamethyl-5-azaporphyrinatoiron(III)], μ-O(FeMAP)$_2$, and μ-oxo-bis[2,8,12,18-tetrabutyl-3,7,13,17-tetramethyl-5,15-diazaporphyrinatoiron(III)], μ-O(FeDAP)$_2$: Solutions of the corresponding free bases H_2MAP or H_2DAP (20 mg, 0.04 mmol) were refluxed in glacial acetic acid (15 mL) in the presence of a 10-fold excess of iron powder (Fluka) for 2–3 h until the disappearance of the free-base absorption bands in the UV/Vis spectra. The reaction mixture was then mixed with an equal volume of $CHCl_3$ and filtered. The filtrate was washed with water until neutral to remove acetic acid, dried with Na_2SO_4 and chromatographed on a column of neutral alumina (Brockmann activity I, eluent $CHCl_3$). In the course of chromatography, the colour of the eluted band changed from red-brown, typical for pentacoordinate mononuclear complexes, to green, characteristic for the binuclear μ-oxo diiron complexes. After evaporation of the solvent the black-green μ-oxo species was obtained in 65–75% yield.

μ-O(FeMAP)$_2$: UV/Vis (benzene): λ_{max} (log ε) = 596 (4.25), 559 (4.09), 420 sh, 361 (4.83) nm. IR (KBr): $\tilde{\nu}_{as}$(Fe–O–Fe) = 890 cm^{-1}. $C_{66}H_{78}Fe_2N_{10}O$ (1139.1): calcd. C 69.59, H 6.90, N 12.30; found C 69.86, H 6.98, N 12.07.

μ-O(FeDAP)$_2$: UV/Vis (benzene): λ_{max} (log ε) = 608 (4.43), 350 (4.65) nm. IR (KBr): $\tilde{\nu}_{as}$(Fe–O–Fe) = 872 cm^{-1}. $C_{76}H_{100}Fe_2N_{12}O$ (1309.4): calcd. C 69.71, H 7.70, N 12.84; found C 69.65, H 7.83, N 12.64.

Acetato(13,17-dibutyl-2,3,7,8,12,18-hexamethyl-5-azaporphyrinato)-iron(III), (AcO)FeMAP, and Acetato(2,8,12,18-tetrabutyl-3,7,13,17-tetramethyl-5,15-diazaporphyrinato)iron(III), (AcO)FeDAP: Glacial acetic acid (0.3 mL) was added to solution of the μ-oxo complex μ-O(FeMAP)$_2$ or μ-O(FeDAP)$_2$ (10 mg, ca. 0.01 mmol) in $CHCl_3$ or benzene (5 mL). The colour of the solution changed from green to red-brown, the mixture was left standing for 30 min and then solvent was evaporated. The residue was washed with hexane to give the corresponding acetate complexes with yield ca. 90%.

(AcO)FeMAP: UV/Vis (benzene): λ_{max} (log ε) = 641 (3.96), 602 (4.00), 548 (4.18), 475 (4.15), 386 sh, 361 (4.92) nm. IR (KBr): $\tilde{\nu}(CO_2)$ = 1274, 1680 cm^{-1}. $C_{35}H_{42}FeN_5O_2$ (620.6): calcd. C 67.74, H 6.82, N 11.28; found C 67.88, H 6.96, N 11.15.

(AcO)FeDAP: UV/Vis (benzene): λ_{max} (log ε) = 678 (3.97), 621 sh, 571 (4.21), 460 (4.18), 343 (4.93) nm. IR (KBr): $\tilde{\nu}(CO_2)$ = 1262, 1664 cm^{-1}. $C_{40}H_{53}FeN_6O_2$ (705.4): calcd. C 68.08, H 7.57, N 11.91; found C 68.26, H 7.67, N 11.80.

Kinetic Measurements: The kinetics of the dissociation of the μ-oxo dimers μ-O(FeMAP)$_2$ and μ-O(FeDAP)$_2$ were studied by using a computer-linked Hitachi U-2000 spectrophotometer equipped with a thermostatted cuvette holder. Benzene solutions of the μ-oxo dimers ($c^0 = 5.1 \times 10^{-5}$ M) and acetic acid (0.01–0.1 M) were preliminary thermostatted at 25, 35 and 45 °C with an accuracy ± 0.05 °C and then mixed together. The changes of the concentration of the complexes in the course of the reaction were followed spectrophotometrically by registration of the optical density at the analytical wavelength: λ = 596 nm for μ-O(FeMAP)$_2$ and λ = 609 nm for μ-O(FeDAP)$_2$. Since the reactions were carried out in a large excess of acetic acid, the observed rate constants of the pseudo first-order reactions were calculated from the changes of optical density A on the analytical wavelengths using equation:

$$k_{obs} = (1/\tau)\ln[(A_0 - A_\infty)/(A_t - A_\infty)] \quad (9)$$

The energy and entropy of activation (E_a and $\Delta S^{\neq}$) were determined from the temperature dependence of k_{obs} using Arrhenius plots.

After evaporation of the solvent from the combined solutions used for kinetic measurements, the corresponding acetate complexes

were obtained. Their spectral characteristics were identical to those obtained in the synthetic procedure described above.

Solution and Refinement of the Structure: X-ray structure analysis of O(FeDAP)$_2$·C$_6$H$_6$: Bruker AXS SMART 1000, CCD-detector λ(Mo-K_a) = 0.71073 Å, graphite monochromator, ω-scanning, $2\theta_{max}$ = 56° at 173(2) K. Corrections for absorption were made by SADABS.[58] The structure was solved by direct method and refined by full-matrix least-squares method for F^2 with anisotropic parameters for all non-hydrogen atoms. The *n*-butyl and methyl groups are disordered at the same sites. One *n*-butyl C(25) atom is disordered over two sites with occupancies 0.5:0.5. All calculations were performed with the use of the SAINT[59] and SHELXTL-97[60] program packages. Crystallographic details are given in Table 6 and selected bond lengths and angles in Tables 1 and 2 and in the caption to Figure 2.

Table 6. Crystallographic data for the structural analysis of μ-O(FeDAP)$_2$·C$_6$H$_6$.

Empirical formula	$C_{82}H_{106}Fe_2N_{12}O$
Formula weight	1387.49
T [K]	173(2)
Crystal system	triclinic
Space group	$P\bar{1}$
a [Å]	14.7134(19)
b [Å]	15.584(2)
c [Å]	18.631(2)
α [°]	98.433(2)
β [°]	108.177(2)
γ [°]	107.874(2)
V [Å^3]	3721.5(8)
Z	2
$D_{calcd.}$ [g cm^{-3}]	1.238
μ [mm^{-1}]	0.444
F(000)	1484
θ range [°]	1.43 to 28.00
Reflections collected	37742
Independent reflections	17834 [R(int) = 0.0724]
Data/restraints/parameters	17834/108/858
$R1$, $wR2[I > 2\sigma(I)]$[a]	0.0685, 0.1715
$R1$, $wR2$ (all data) [a]	0.1369, 0.2006
GoF	1.062
$\Delta\rho$(max), $\Delta\rho$ [min] [e Å^{-3}]	1.544, –1.241

[a] $R_1 = \Sigma||F_o| - |F_c||/\Sigma|F_o|$; $wR_2 = \{\Sigma[w(F_o^2 - F_c^2)^2]/\Sigma w(F_o^2)^2\}^{1/2}$.

CCDC-801543 contains the supplementary crystallographic data for for μ-O(FeDAP)$_2$·C$_6$H$_6$. These data can be obtained free of charge from The Cambridge Crystallographic Data Centre via www.ccdc.cam.ac.uk/data_request/cif.

Supporting Information (see footnote on the first page of this article): X-ray data crystallographic and structural refinement data for μ-O(FeDAP)$_2$·C$_6$H$_6$.

Acknowledgments

This work was supported partly by Russian Foundation of Basic Research (grant number 10-03-00967) and by Russian Federal Agency of Science and Innovations (grant number 02.740.11.0106). We are thankful to Prof. A. S. Semeikin and Dr. S. S. Ivanova for preparation of the free bases (H_2MAP and H_2DAP).

[1] S. V. Barkanova, V. M. Derkacheva, I. A. Zheltukhin, O. L. Kaliya, E. A. Lukyanets, *Zh. Org. Khim.* **1985**, *21*, 2018–2019.
[2] a) I. M. Geraskin, M. W. Luedtke, H. M. Neu, V. N. Nemykin, V. V. Zhdankin, *Tetrahedron Lett.* **2008**, *49*, 7410–7412; b) H. M. Neu, M. S. Yusubov, V. V. Zhdankin, V. N. Nemykin, *Adv. Synth. Catal.* **2009**, *351*, 3168–3174; c) H. M. Neu, V. V. Zhdankin, V. N. Nemykin, *Tetrahedron Lett.* **2010**, *51*, 6545–6548.
[3] a) P. E. J. Ellis, J. E. Lyons, *J. Chem. Soc., Chem. Commun.* **1989**, 1315–1316; b) P. E. J. Ellis, J. E. Lyons, *Coord. Chem. Rev.* **1990**, *105*, 181–193.
[4] a) L. Weber, G. Haufe, D. Rehorek, H. Hennig, *J. Chem. Soc., Chem. Commun.* **1991**, 502–503; b) S. Srinivasan, W. T. Ford, *J. Mol. Catal.* **1991**, *64*, 291.
[5] a) H.-Y. Hu, Q. Jiang, Q. Liu, J.-X. Song, W.-Y. Ling, C.-C. Guo, *J. Porphyrins Phthalocyanines* **2006**, *10*, 948–952; b) X.-T. Zhou, Q.-H. Tang, H.-B. Ji, *Tetrahedron Lett.* **2009**, *50*, 6601.
[6] D. G. Nocera, *Abstracts of Papers*, 234th ACS National Meeting, Boston, MA, USA, August 19–23, **2007**, INOR-463.
[7] a) S. K. Ghosh, R. Patra, S. P. Rath, *Inorg. Chem.* **2008**, *47*, 10196–10198; b) R. Patra, S. Bhowmik, S. K. Ghosh, S. P. Rath, *Eur. J. Inorg. Chem.* **2009**, 654–665; c) S. K. Ghosh, R. Patra, S. P. Rath, *Inorg. Chim. Acta* **2010**, *363*, 2791–2799; d) S. K. Ghosh, R. Patra, S. P. Rath, *Inorg. Chem.* **2010**, *49*, 3449–3460.
[8] O. A. Golubchikov, B. D. Berezin, I. M. Kazakova, M. B. Berezin, *Zh. Obshch. Khim.* **1982**, *52*, 83–90.
[9] P. A. Stuzhin, M. Hamdush, B. D. Berezin, *Zh. Fiz. Khim.* **1996**, *70*, 807–814; *Russ. J. Phys. Chem.* **1996**, *70*, 747–753.
[10] J. W. Buchler, H. H. Schneehage, *Z. Naturforsch., Teil B* **1973**, *28*, 433–439.
[11] G. N. La Mar, G. R. Eaton, R. H. Holm, F. A. Walker, *J. Am. Chem. Soc.* **1973**, *95*, 63–75.
[12] N. V. Ivashin, A. M. Shul'ga, S. N. Terekhov, K. Dzilin'ski, *Zh. Prikl. Spektrosk.* **1994**, *61*, 72–82.
[13] N. V. Ivashin, A. M. Shul'ga, S. N. Terekhov, K. Dzilin'ski, *Spectrochim. Acta A* **1996**, *52A*, 1603–1614.
[14] J. P. Fitzgerald, B. S. Haggerty, A. L. Rheingold, L. May, G. A. Brewer, *Inorg. Chem.* **1992**, *31*, 2006–2013.
[15] S. Saito, S. Sumita, K. Iwai, H. Sano, *Bull. Chem. Soc. Jpn.* **1988**, *61*, 3539–3547.
[16] K. Dzilin'ski, G. N. Sinyakov, A. M. Shul'ga, *Zh. Prikl. Spektr.* **1999**, *66*, 515–518 (Russ.*); J. Appl. Spectrosc.* **1999**, *66*, 566–569 *(Engl.)*.
[17] A. L. Balch, M. M. Olmstead, N. Safari, *Inorg. Chem.* **1993**, *32*, 291–296.
[18] K. Dzilinski, T. Kaczmarzyk, T. Jackowski, G. N. Sinyakov, G. D. Egorova, *Mol. Phys. Rep.* **2003**, *37*, 35–41.
[19] K. Nakamura, A. Ikezaki, Y. Ohgo, M. Nakamura, T. Ikeue, S. Neya, *Inorg. Chem.* **2008**, *47*, 10299–10307.
[20] S. Neya, H. Hori, K. Imai, Y. Kawamura-Konishi, H. Suzuki, Y. Shiro, T. Iizuka, N. Funasaki, *J. Biochem. (Tokyo)* **1997**, *121*, 654–660.
[21] Y. Ohgo, S. Neya, H. Uekusa, M. Nakamura, *Chem. Commun.* **2006**, *44*, 4590–4592.
[22] P. A. Stuzhin, S. E. Nefedov, R. S. Kumeev, A. Ul-Haq, V. V. Minin, S. S. Ivanova, *Inorg. Chem.* **2010**, *49*,(11) 4802–4813; DOI: 10.1021/ic9012075.
[23] P. A. Stuzhin, *Macroheterocycles*, **2009**, *2*, 114–129 [http://macroheterocycles.isuct.ru/sites/default/files/MHC2009t02n02_114–129_0.pdf].
[24] W. R. Scheidt, C. A. Reed, *Chem. Rev.* **1981**, *81*, 543–555.
[25] A. B. Hoffman, D. M. Collins, V. W. Day, E. B. Fleischer, T. S. Srivastava, J. L. Hoard, *J. Am. Chem. Soc.* **1972**, *94*, 3620–3626.
[26] a) A. L. Litvinov, D. V. Konarev, A. Y. Kovalevsky, A. N. Lapshin, N. V. Drichko, E. I. Yudanova, P. Coppens, R. N. Lyubovskaya, *Eur. J. Inorg. Chem.* **2003**, 3914–3917; b) D. V. Konarev, S. S. Khasanov, R. N. Lyubovskaya, *J. Porphyrins Phthalocyanines* **2010**, *14*, 293–297.
[27] B. Cheng, J. D. Hobbs, P. G. Debrunner, J. Erlebacher, J. A. Shelnutt, W. R. Scheidt, *Inorg. Chem.* **1995**, *34*, 102–110.
[28] H. M. Lee, M. M. Olmstead, G. G. Gross, A. L. Balch, *Cryst. Growth Des.* **2003**, *3*, 691–697.

[29] W. R. Scheidt, B. Cheng, M. K. Safo, F. Cukernik, J.-C. Marchon, P. G. Debrunner, *J. Am. Chem. Soc.* **1992**, *114*, 4420–4421.
[30] W. R. Scheidt, Y. J. Lee, *Struct. Bonding (Berlin)* **1987**, *64*, 1–70.
[31] P. A. Stuzhin, M. Goeldner, H. Homborg, A. S. Semeikin, I. S. Migalova, S. Wolowiec, *Mendeleev Commun.* **1999**, 134–136.
[32] I. A. Cohen, *J. Am. Chem. Soc.* **1969**, *91*, 1980–1983.
[33] P. A. Stuzhin, I. S. Migalova, B. D. Berezin, *Zh. Neorg. Khim.* **1998**, *43*, 1655–1660.
[34] G. Fitzgerald, W. Taylor, H. Owen, *Synthesis* **1991**, 686–688.
[35] P. A. Stuzhin, S. S. Ivanova, I. S. Migalova, *Zh. Obshch. Khim.* **2004**, *74*, 1546–1556; *Russ. J. Gen. Chem.* **2004**, *74*, 1435–1445.
[36] G. N. La Mar, F. A. Walker in *The Porphyrins*, (Eds.: D. Dolphin), Academic Press, New York, **1979**, vol. IV, p. 57–161.
[37] F. A. Walker, in: *The Porphyrin Handbook* (Eds: K. M. Kadish, K. M. Smith, R. Guilard), Academic Press, Amsterdam, **2000**, vol. 5, p. 81–183.
[38] H. Lueken, J. W. Buchler, K. L. Lay, *Z. Naturforsch., Teil B* **1976**, *31*, 1596–1603.
[39] S. S. Dvornikov, V. N. Knyukshto, V. A. Kuzmitski, A. M. Shulga, K. N. Solovyov, *J. Lumin.* **1981**, *23*, 373–392.
[40] H. Ogata, T. Fukuda, K. Nakai, Y. Fujimura, S. Neya, P. A. Stuzhin, N. Kobayashi, *Eur. J. Inorg. Chem.* **2004**, *8*, 1621–1629.
[41] P. A. Stuzhin, A. Ul-Hak, N. V. Chizhova, A. S. Semeikin, *Zh. Fiz. Khim.* **1998**, *72*, 1585–1591.
[42] O. G. Khelevina, N. V. Chizhova, P. A. Stuzhin, A. S. Semeikin, B. D. Berezin, *Koord. Khim.* **1996**, *22*, 866–869; *Russ. J. Coord. Chem.* **1996**, *22*, 807–814.
[43] M. Gouterman, D. Holten, E. Lieberman, *Chem. Phys.* **1977**, *25*, 139–153.
[44] P. A. Stuzhin, M. Hamdush, U. Ziener, *Inorg. Chim. Acta* **1995**, *236*, 131–139.
[45] B. J. Kennedy, K. S. Murray, P. R. Zwack, H. Homborg, W. Kalz, *Inorg. Chem.* **1986**, *25*, 2539–2545.
[46] I. Morishima, S. Kitagawa, E. Matsuki, T. Inubushi, *J. Am. Chem. Soc.* **1980**, *102*, 2429–2437.
[47] W. D. Edwards, B. Weiner, M. C. Zerner, *J. Phys. Chem.* **1988**, *92*, 6188–6197.
[48] H. Oumous, C. Lecomte, J. Protas, P. Cocolios, R. Guilard, *Polyhedron* **1984**, *3*, 651–659
[49] K. Nakamoto, *Infrared and Raman Spectra of Inorganic and Coordination Compounds*, John Wiley & Sons, New York, **1986**, p. 478.
[50] H. M. Goff, in: *Iron Porphyrins* (Eds.: A. B. P. Lever, H. B. Gray), Addison-Wesley, Reading, U.K., **1983**, part 1, p. 237–281.
[51] N. S. Zaugg, A. J. Kelley, E. M. Wooley, *J. Chem. Eng. Data* **1979**, *24*, 218.
[52] Y. Fujii, H. Yamada, M. Mizuta, *J. Phys. Chem.* **1988**, *92*, 6768–6772.
[53] M. M. Davis, M. Paabo, *J. Org. Chem.* **1966**, *31*, 1804–1810.
[54] P. Chaudhuri, K. Wieghardt, B. Nuber, J. Weiss, *Angew. Chem.* **1985**, *97*, 774–775.
[55] W. H. Armstrong, S. J. Lippard, *J. Am. Chem. Soc.* **1984**, *106*, 4632–4633.
[56] P. A. Stuzhin, A. Ul'-Khak, N. V. Chizhova, A. S. Semeikin, O. G. Khelevina, *Zh. Fiz. Khim.* **1998**, *72*, 1585–1591.
[57] O. G. Khelevina, N. V. Chizhova, P. A. Stuzhin, A. S. Semeikin, B. D. Berezin, *Zh. Fiz. Khim.* **1997**, *71*, 81–85; *Russ. J. Phys. Chem.* **1997**, *71*, 74–78.
[58] G. M. Sheldrick, *SADABS*, **1997**, Bruker AXS Inc., Madison, WI-53719, USA.
[59] *SMART*, v. 5.051 and *SAINT*, v. 5.00; area detector control and integration software, **1998**, Bruker AXS Inc., Madison, WI-53719, USA.
[60] G. M. Sheldrick, *SHELXTL-97*, v. 5.10, **1997**, Bruker AXS Inc., Madison, WI-53719, USA.

Received: February 1, 2011
Published Online: April 29, 2011

